[Channels 1:2, 80-91; March/April 2007]; ©2007 Landes Bioscience

Research Paper

An NH2-Terminal Multi-Basic RKR Motif Is Required for the ATP-Dependent Regulation of hIK1

Heather M. Jones[1,2]
Mark A. Bailey[1]
Catherine J. Baty[1]
Gordon G. MacGregor[1]
Colin A. Syme[1]
Kirk L. Hamilton[3]
Daniel C. Devor[1,*]

[1]Department of Cell Biology and Physiology; University of Pittsburgh; Pittsburgh, Pennsylvania USA

[2]Present Address: Department of Biology; School of Science; Penn State Erie; The Behrend College; Erie, Pennsylvania USA

[3]Department of Physiology; University of Otago; Dunedin, New Zealand

[*]Correspondence to: Daniel C. Devor, Ph.D.; Department of Cell Biology and Physiology; University of Pittsburgh School of Medicine; S312 BST; 3500 Terrace Street; Pittsburgh, Pennsylvania 15261, USA; Tel.: 412.383.8755; Fax: 412.648.8330; Email: dd2@pitt.edu

Original manuscript submitted: 11/15/06
Revised manuscript submitted: 02/12/07
Manuscript accepted: 02/12/07

Previously published online as a *Channels* E-Publication:
http://www.landesbioscience.com/journals/channels/article/3999

KEY WORDS

hIK1, KCa3.1, regulation, potassium channel, trafficking

ACKNOWLEDGEMENTS

This work was supported by a National Institutes of Health grants (DK54941, HL083060) to Daniel C. Devor, a National Institute of Health T32 training grant (DK061296-03) to Heather M. Jones, the University of Otago (Department of Physiology) for sabbatical support of Kirk L. Hamilton and a postdoctoral fellowship (AHA 0120544U) to Colin A. Syme.

ABSTRACT

We previously demonstrated that the ATP/PKA-dependent activation of the human intermediate conductance, Ca^{2+}-activated K^+ channel, hIK1, is dependent upon a C-terminal motif. The NH_2-terminus of hIK1 contains a multi-basic ^{13}RRRKR^{17} motif, known to be important in the trafficking and function of ion channels. While individual mutations within this domain have no effect on channel function, the triple mutation (^{15}RKR^{17}/AAA), as well as additional double mutations, result in a near complete loss of functional channels, as assessed by whole-cell patch-clamp. However, cell-surface immunoprecipitation studies confirmed expression of these mutated channels at the plasma membrane. To elucidate the functional consequences of the ^{15}RKR^{17}/AAA mutation we performed inside-out patch clamp recordings where we observed no difference in Ca^{2+} affinity between the wild-type and mutated channels. However, in contrast to wild-type hIK1, channels expressing the ^{15}RKR^{17}/AAA mutation exhibited rundown, which could not be reversed by the addition of ATP. Wild-type hIK1 channel activity was reduced by alkaline phosphatase both in the presence and absence of ATP, indicative of a phosphorylation event, whereas the ^{15}RKR^{17}/AAA mutation eliminated this effect of alkaline phosphatase. Further, single channel analysis demonstrated that the ^{15}RKR^{17}/AAA mutation resulted in a four-fold lower channel open probability (P_o), in the presence of saturating Ca^{2+} and ATP, compared to wild-type hIK1. In conclusion, these results represent the first demonstration for a role of the NH_2-terminus in the second messenger-dependent regulation of hIK1 and, in combination with our previous findings, suggest that this regulation is dependent upon a close NH_2/C-terminal association.

INTRODUCTION

The human intermediate conductance, Ca^{2+}-activated K^+ channel (hIK1) is known to play crucial roles in a wide array of physiological processes.[1-6] To fully appreciate the role of these channels in eliciting these physiological effects requires an understanding of the regulatory pathways involved in channel activation and inhibition. Recent reports have highlighted the role of the cytoplasmic C-terminus in both second messenger-dependent regulation and trafficking of hIK1. Indeed, the calmodulin binding domain,[7,8] ATP/PKA-dependent regulatory domain[9,10] and PKC-dependent regulatory domain[11] have all been mapped to the C-terminus of hIK1. In addition to these regulatory domains, Joiner et al,[12] demonstrated that the binding of calmodulin to the proximal C-terminal tail of hIK1 was required for the efficient assembly and trafficking of hIK1 to the plasma membrane. Recently, our laboratory demonstrated that a leucine zipper in the distal C-terminal tail of hIK1 was required for correct trafficking of hIK1 to the cell surface and that this effect was likely due to the self-assembly of the leucine zipper into a coiled-coil domain.[13]

In contrast to these studies on the C-terminus of hIK1, the role of the cytoplasmic NH_2-terminus in the regulation and trafficking of hIK1 has been little studied. We recently demonstrated that the NH_2-terminus contains a series of leucines critical to channel tetramerization and trafficking.[14] In addition to this hydrophobic domain, the NH_2-terminus of hIK1 also includes a multi-basic motif (^{13}RRRKR^{17}). Multi-basic motifs have been shown to be important in ER retention/retrieval of K_{ATP} channels and the $GABA_B$ receptor[15,16] as well as ER exit and basolateral sorting of the betaine transporter in epithelial cells.[17] Importantly, NH_2-terminal basic clusters have also been shown to be critical in controlling the gating of K^+ channels, including ROMK[18] and K_{ATP}.[19] To date, no second messenger-dependent regulatory domains have been mapped to the NH_2-terminus of hIK1.

In the present study we investigated the role of this NH_2-terminal RKR motif in the trafficking and function of hIK1. We demonstrate that alanine mutations within the RKR domain do not abrogate cell surface expression of hIK1, indicating this multi-basic motif is not required for trafficking of the channel to the plasma membrane. In contrast, we demonstrate, using whole-cell and inside-out patch-clamp techniques, that the ATP-dependent regulation of hIK1 is abolished following mutation of the NH_2-terminal RKR motif with no change in apparent Ca^{2+} affinity. This abolition of ATP dependence results in the mutated channel having a dramatically reduced open probability (P_o) compared to wild-type hIK1. These results represent the first demonstration for a role of the NH_2-terminus in the regulation of hIK1.

EXPERIMENTAL PROCEDURES

Molecular biology. pBF plasmid containing the cDNA for full-length hIK1 cDNA was kindly provided by J.P. Adelman (Vollum Institute, Oregon Health Sciences University). hIK1 was subcloned into pcDNA3.1(+) (Invitrogen, Carlsbad, CA) using the *EcoRI* and *XhoI* restriction sites. A hemagglutinin (HA; YPYDVPDYA) epitope was inserted into hIK1 (HA-hIK1) between G132 and A133, i.e., the extracellular loop between transmembrane domains S3 and S4, by sequential overlap extension PCR, as described previously.[13] An HA tag was appended to the C-terminus of hIK1 (HA-C-Term) in a single-step PCR. hIK1 was tagged with a C-terminal *myc*-epitope (EQKLISEEDL) through PCR amplification as described.[13] All mutations in hIK1 (R15A/K16A/R17A (RKR/AAA), R13A, R14A, R15A, K16A, R17A, R13A/R14A, R15A/K16A and R15A/R17A) were generated using the Stratagene QuikChangeä site-directed mutagenesis strategy (Stratagene, La Jolla, CA). The fidelity of all constructs utilized in this study was confirmed by sequencing (ABI PRISM 377 automated sequencer, University of Pittsburgh) and subsequent sequence alignment (NCBI BLAST) with hIK1 (GenBank™ accession number AF022150).

Cell culture. Human embryonic kidney (HEK293) cells were obtained from the American Type Culture Collection (Manassas, VA) and cultured in Dulbecco's modified Eagle's medium (DMEM; Invitrogen) supplemented with 10% fetal bovine serum and 1% penicillin-streptomycin in a humidified 5% CO_2/95% O_2 incubator at 37°C. Cells were transfected using LipofectAMINE 2000 (Invitrogen) following the manufacturer's instructions. Stable cell lines were generated for all constructs by subjecting cells to antibiotic selection (1mg/ml G418). Note that clonal cell lines were not subsequently selected from this stable population in order to avoid clonal variation.

Electrophysiology. During whole-cell patch-clamp experiments the bath contained (in mM) 140 NaCl, 4 KCl, 2 $CaCl_2$, 1 $MgCl_2$, and 10 HEPES (pH adjusted to 7.4 with NaOH). The pipette solution contained (in mM) 130 KCl, 5 NaCl, 0.12 $CaCl_2$, 4 $MgCl_2$, 10 HEPES, and 0.2 EGTA (pH adjusted to 7.2 with KOH) this gives a calculated free-Ca^{2+} concentration of 200 nM. All experiments were performed at room temperature (22°C) using stably transfected HEK293 cells plated the previous day. Electrodes were fabricated from thin-walled borosilicate glass (World Precision Instruments, Sarasota, FL), pulled on a vertical puller (Narishige, Long Island, NY). Currents were recorded using an Axon Instruments 200B amplifier (Axon Instruments, Foster City, CA) interfaced to a computer using a Digidata 1322A (Axon Instruments). Following establishment of the whole-cell configuration, voltage steps (250 ms duration) were applied between -100 to +80 mV from a holding potential of -60 mV in 20 mV increments to generate a current-voltage (I-V) relationship using pCLAMP 8.2 software (Axon Instruments). Current was sampled at steady-state (100 msec) for the purpose of evaluating current density. Current density (pA/pF) at zero mV was calculated by dividing the current by the whole cell capacitance. Similar I-Vs were generated following stimulation with 10 μM DCEBIO (5,6-dichloro-1-ethyl-1,3-dihydro-2H-benzimidazol-2-one;[20] and inhibition with the hIK1 blocker, clotrimazole (CLT; 3 μM). The current densities reported throughout the manuscript are the clotrimazole-inhibited currents. This ensures that if any baseline current is due to hIK1 it will be accounted for in the measurements reported.

Inside-out patch-clamp experiments. The effects of Ca^{2+}, DCEBIO, ATP and alkaline phosphatase on hIK1 were assessed with excised, inside-out patch-clamp experiments as a functional assay. During patch-clamp experiments, the bath solution contained 145 mM K-gluconate, 5 mM KCl, 2 mM $MgCl_2$, 10 mM HEPES and 1 mM EGTA (pH adjusted to 7.2 with KOH). Sufficient $CaCl_2$ was added to obtain the desired free Ca^{2+} concentration (program kindly provided by Dr. Dave Dawson, Oregon Health Sciences University). To obtain a 0 Ca^{2+} bath solution EGTA (1 mM) was added without $CaCl_2$ (estimated free Ca^{2+} < 10 nM). The pipette solution was 140 mM K-gluconate, 5 mM KCl, 1 mM $MgCl_2$, 10 mM HEPES and 1 mM $CaCl_2$ (pH adjusted to 7.2 with KOH). All experiments were performed at room temperature. All patches were held at a holding potential of -100 mV. The voltage is referenced to the extracellular compartment, as is the standard method for membrane potentials. Inward currents are defined as the movement of positive charge from the extracellular compartment to the intracellular compartment and are presented as downward deflections from the baseline in all recordings. Immediate bath solution changes were achieved using Automate Scientifics' (San Francisco, CA) pressurized perfusion system and recordings were continuous to allow for the most rapid changes in current to be recorded. Single channel analysis was performed on records after low pass filtering at 400 Hz and sampling at 1 KHz. Total channel current was determined using Biopatch software (version 3.3, Bio-Logic) or Clampfit 8.2 (Axon Instruments).

Variance analysis. Excised patch-clamp recordings that were subject to variance analysis were filtered at 10kHz and digitized at 20kHz. For these studies, current recordings were initiated immediately following patch excision into a bath containing 10 μM free Ca^{2+}, but lacking ATP. Following channel rundown the channels were reactivated with ATP (300 μM) and subsequently DCEBIO (10 μM). The total current record was divided into 250 episodes and mean current (I) and variance (σ^2) were calculated for each episode using Channelab Software (Synaptosoft Inc., Decatur, GA, USA). The number of channels (N) in the patch and single channel amplitude (i) are obtained by fitting the variance (σ^2) against mean current (I) distribution to Equation 1:

$$\sigma^2 = iI - \frac{I^2}{N} \quad (1)$$

The maximum open probability (P_{omax}) can then be calculated using Equation 2:

$$Po_{max} = \frac{I_{max}}{iN} \quad (2)$$

where, I_{max} is the maximum current observed and i and N are the mean values for single channel amplitude and number of channels calculated from Equation 1. The product of i and N would give the theoretical current at $P_o = 1$, hence, channel P_o can be calculated at any given current as a proportion of P_{omax}.[21-24]

Single channel analysis. Amplitude histograms were compiled from 2 to 3 minutes of current trace binned in 0.1 pA intervals using pClamp8.0. To calculate P_o, we initially calculated the area under each peak in the amplitude histogram (i.e., the total time spent at a current level) using Equation 3:

$$f(x) = \sum_{i=0}^{n} A_i \frac{1}{\sigma_i \sqrt{2\pi}} \exp\left\{-\frac{(x-\mu_i)^2}{2\sigma_i^2}\right\} \quad (3)$$

where: i = 0, 1, 2, 3,……..n, are the individual current levels, A is the area under peak i, μ is the mean of the Gaussian peak i and σ is the Gaussian standard deviation. The area under each peak is normalized to the total area under the amplitude histogram, giving the probability of appearing in level i (P_i), where i = 0, 1, 2, 3…..n. The channel P_o is calculated as NP_o/n, where NP_o is:

$$NPo = \sum_{i=0}^{n} iP_i \quad (4)$$

where *n* is the predicted number of channels in the patch. We estimated *n* from the highest peak observed in the amplitude histogram under stimulation with DCEBIO. We are confident in our calculation of the total number of channels in a patch (n) as each individual level probability (P_i) is in very good agreement with a binomial distribution (see Equation 5) for the appropriate number of channels:

$$P_i = \frac{n!}{i!(n-i)!} p^i (1-p)^{n-i} \quad (5)$$

where, n is the number of independent channels in the patch and i is the integer number of the amplitude histogram level (where the closed state is now level 0) and the equation is solved for *p*, the open channel probability.

Antibodies. To detect hIK1 in immunoprecipitation (IP) and immunoblotting (IB) experiments, antibodies were obtained from the following sources (dilutions used are indicated): polyclonal HA (1:150) and monoclonal (1:1,000) HA (HA.11, Covance, Richmond, CA), *c-myc* (clone 9E10, 1:1,000; Roche Molecular Biochemicals, Indianapolis, IN), HRP-conjugated goat anti-mouse IgG (1:2,000; KPL, Gaithersburg, MD) and HRP-conjugated goat anti-rabbit IgG (1:2,000; Transduction Laboratories, San Diego, CA).

Immunoprecipitation (IP). For cell-surface IP (CS-IP), cells were grown to confluence in a 100 mm dish, washed in ice-cold PBS, blocked in 1% BSA/PBS and labeled with polyclonal HA.11 Ab (1:500) for 90 mins at 4°C. Unbound Ab was removed by extensive washing in 1% BSA followed by washes in PBS. All steps were performed at 4°C to prevent endocytosis of the channel and/or Ab. The cells were then lysed in IP buffer (50 mM HEPES pH 7.4, 150 mM NaCl, 1% v/v Triton X-100, 1 mM EDTA containing Complete™ EDTA-free protease inhibitor cocktail mix, Roche). Protein concentrations were determined and normalized to achieve equivalent loading. Crude lysates were pre-cleared with protein A-sepharose beads (Sigma-Aldrich, St. Louis, MO) and incubated with rabbit polyclonal anti-HA antibody. Immune complexes were precipitated with protein A-sepharose beads, followed by sequential washes in IP buffer containing 500 mM, 300 mM, and 150 mM (2x) NaCl, supplemented with 1x radioimmunoprecipitation assay (RIPA) buffer (50 mM Tris-HCl pH 7.5, 150 mM NaCl, 1% v/v Triton X-100, 1% w/v sodium deoxycholate, and 0.1% w/v SDS). After the final wash, the pellet was resuspended in Laemmli sample buffer, proteins resolved by SDS-PAGE (12% gel) and transferred to nitrocellulose for immunoblot analysis using monoclonal HA Ab (1:1,000) as detailed below. As a control for intracellular labeling we utilized a channel in which the HA epitope was added to the cytoplasmic C-terminus. While this channel is expressed at high levels at the cell surface it can not be labeled in these studies unless the HA Ab has access to an intracellular compartment.

Immunoblot analysis. HEK293 cells were grown to confluence, lysed with IP buffer, separated by SDS-PAGE electrophoresis, and transferred to nitrocellulose. Blots were blocked for one hour at room temperature using TBS-blocking solution containing 5% w/v milk powder, 0.1% (v/v) Tween-20, 0.005% (v/v) Antifoam A. Subsequently, blots were incubated in 1° Ab (mouse monoclonal HA, 1:1,000) for one hour at room temperature, extensively washed (TBS-blocking solution deficient in milk powder) followed by incubation in 2° Ab (1:2,000; HRP-conjugated goat anti-mouse IgG). The blot was then extensively washed and detection performed using West Pico Chemiluminescent Substrate (Pierce, Rockford, IL).

Chemicals. All chemicals were obtained from Sigma-Aldrich, unless otherwise stated. DCEBIO was synthesized in the laboratory of R.J. Bridges (University of Pittsburgh), as previously described.[20] Both DCEBIO and clotrimazole were made as 10,000-fold stock solutions in DMSO. Complete EDTA-free protease inhibitor cocktail mix was obtained from Roche Molecular Biochemicals.

Statistics. All data are presented as means ± SEM, where n indicates the number of experiments. Statistical analysis was performed using a Student's t test. A value of $p < 0.05$ is considered statistically significant and is reported. All protein biochemical experiments were carried out minimally three times on each construct to ensure the voracity of our results.

RESULTS

An NH_2-terminal multi-sasic RKR motif is required for the functional expression of hIK1. While the predicted NH_2-terminus of hIK1 is only 26 amino acids long it contains a series of potentially important molecular motifs required for proper channel assembly, trafficking and function. We previously demonstrated that the NH_2-terminus of hIK1 contains a series of leucine residues required for both tetramerization as well as trafficking to the cell surface.[14] In addition to these hydrophobic amino acids, the NH_2-terminus of hIK1 contains a multi-basic ^{13}RRRKR^{17} motif; a motif previously shown to be important in ER retention,[15,16] ER exit[17] and channel gating.[18,19] To evaluate the role of this multi-basic motif in hIK1 we engineered a series of single, double and triple alanine-substituted mutations and determined both cell surface expression and function. Functional expression was evaluated by determining the DCEBIO-stimulated, clotrimazole-inhibited whole-cell current density (pA/pF), whereas cell surface expression was determined by CS-IP, as previously described.[13,14] In wild-type hIK1 expressing cells, DCEBIO (10 μM) increased the whole-cell current as

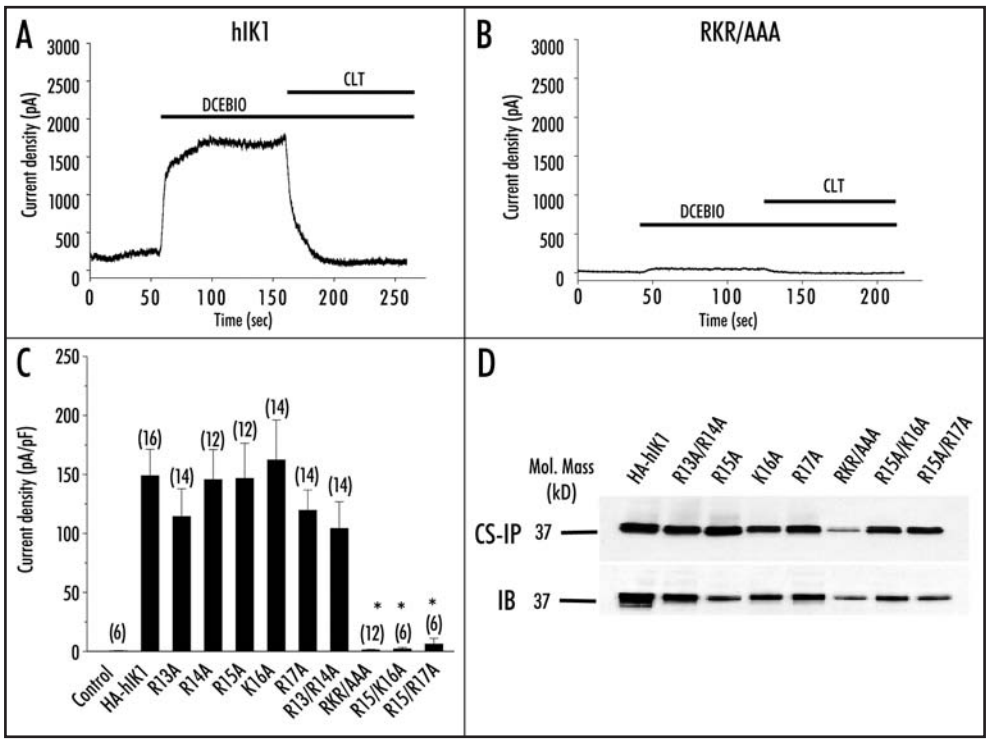

Figure 1. Mutation of the NH_2-terminal RKR motif compromises function of hIK1. Representative whole-cell current traces from (A) HA-hIK1 or (B) RKR/AAA stably transfected in HEK293 cells in response to 10 μM DCEBIO and 3 μM clotrimazole. (C) Average DCEBIO-stimulated (10 μM), clotrimazole-sensitive (3 μM) current densities (pA/pF) plotted for each construct at -20 mV. The number of experiments is indicated in parenthesis. The asterisks indicate statistical significance ($p < 0.05$). (D) Cell Surface Immunoprecipitation (CS-IP) of HA-hIK1 channel constructs. (Top panel) CS-IP confirms expression of HA-hIK1, R13A/R14A, R15A, K16A, R17A, RKR/AAA, R15A/K16A and R15A/R17A at the cell surface of HEK293 cells. (Bottom panel) Immunoblot (20 μg total protein) indicating the cellular levels of IK1 channel expression for all constructs. The immunoblots shown are representative of three separate experiments.

shown in Figure 1A. This current was subsequently inhibited by clotrimazole (3 μM) to near baseline. For all whole-cell recordings an average clotrimazole-inhibited current density of 149 ± 22 pA/pF (n = 16, Fig. 1C) was recorded for wild-type hIK1 channels, which represents a 610 ± 90% increase in current by DCEBIO. As shown in Figure 1C, individually mutating each of the ^{13}RRRKR^{17} residues to alanine failed to affect the DCEBIO-stimulated, clotrimazole-inhibited current density (R13A, 114 ± 23 pA/pF, n = 14; R14A, 146 ± 25 pA/pF, n = 12; R15A, 147 ± 30 pA/pF, n = 12; K16A, 162 ± 34 pA/pF, n = 14; R17A, 120 ± 17 pA/pF, n = 14). Similarly, the double mutation, R13A/R14A had no effect on total clotrimazole-inhibited current density (104 ± 23 pA/pF, n = 14). In contrast to these results, a triple mutation of the ^{15}RKR^{17} motif to alanines (RKR/AAA) resulted in a greatly diminished DCEBIO-stimulated, clotrimazole-inhibited response when compared to the wild-type channel (Fig. 1B); having an average current density of 1.3 ± 0.4 pA/pF (n = 12; Fig. 1C), which represents only a 20 ± 20% increase in current by DCEBIO. Similar reductions in clotrimazole-inhibited current densities were seen with the double mutations R15A/K16A (2.0 ± 1.3 pA/pF, n = 6; $p < 0.05$) and R15A/R17A (6.2 ± 4.9 pA/pF, n = 6; $p < 0.05$). These results demonstrate a clear role for this RKR motif in the functional expression of hIK1.

While the above results demonstrate a lack of functional expression following mutation of the NH_2-terminal RKR motif, they do not distinguish between the possibility that hIK1 is expressed at the cell surface and is non-functional versus hIK1 fails to traffic to the cell surface following mutation of this RKR motif. We previously demonstrated that insertion of an HA epitope into the second extracellular domain of hIK1 allows us to monitor cell surface expression by CS-IP while having no effect on the biophysical or regulatory properties of the channel.[13] Thus, we performed CS-IP to evaluate the possibility that the RKR/AAA, R15A/K16A and R15A/R17A mutations fail to express at the cell surface. As shown in Figure 1D, HA-hIK1 is expressed at the cell surface (lane 1). In contrast to our functional data, all of the alanine-substituted mutations expressed at the cell surface at levels similar to wild-type, except the RKR/AAA mutation (lane 6), which was reduced to an average of 21% of wild-type (n = 4), as determined by densitometry. Thus, this 4.7 ± 2.2-fold decrease in cell surface expression cannot explain the 30-fold decrease in stimulated current observed between wild-type and RKR/AAA expressing cells. Also, a similar decrease in current density was observed for the R15A/K16A and R15A/R17A mutations, channels that exhibit a cell surface expression level similar to wild-type hIK1.

Given this reduction in cell surface expression of the RKR/AAA mutation, we determined whether incubating the cells at reduced temperature (27°C), in butyrate (5 mM) or both could increase expression. We,[13] and others[25-27] have previously shown that incubating cells at 27°C or in the presence of butyrate can increase expression of trafficking compromised channels. As shown in Figure 2A, reducing the incubation temperature to 27°C in the presence or absence of butyrate increased the cell surface expression of the RKR/AAA channel. As a control for this assay, we demonstrate that a hIK1 channel tagged with a HA epitope at the cytoplasmic C-terminus (HA-C-term) was not detected by cell surface IP, as would be expected for an intracellular localized epitope. However, as shown in the immunoblot (Fig. 2A), HA-C-term is highly expressed in these cells. Indeed, even though 10-fold less total

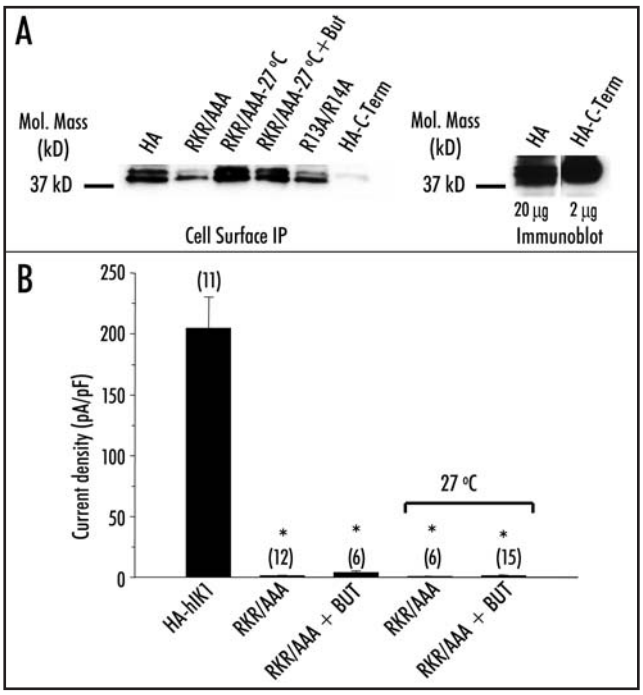

Figure 2. Reduced incubation temperature increases expression but not function of RKR/AAA-HA-hIK1. (A, left panel) Cell surface immunoprecipitation of HA-hIK1 (lane 1), RKR/AAA grown at 37°C (lane 2), RKR/AAA grown at 27°C (lane 3), RKR/AAA grown at 27°C in the presence of 5 mM butyrate (lane 4), R13A/R14A (lane 5) and a C-terminal HA-tagged construct (lane 6). (A, right panel) Immunoblot of HA-hIK1 (20 µg total protein) and HA-C-Term (2 µg total protein). Reduced incubation temperature (27°C) increases cell surface expression of RKR/AAA-HA-hIK1. HA-C-Term was not detected during cell surface IP confirming that only cell surface epitope is recognized. Similar results were obtained in three separate experiments. (B) Average DCEBIO-stimulated, clotrimazole-sensitive current density (pA/pF) for each construct at -20 mV. The number of experiments is indicated in parenthesis. Asterisks indicate statistical significance ($p < 0.05$).

protein was loaded (2 µg vs. 20 µg) we detected a similar signal on IB for HA-C-term compared to HA-hIK1. Whether this difference is due to a true 10-fold difference in expression or a difference in epitope recognition it clearly demonstrates the selective nature of our CS-IP experiments for an extracellular epitope. Despite this increased expression at the cell surface, the RKR/AAA channels failed to express functionally, as assessed by DCEBIO-stimulated, clotrimazole-sensitive current density measurements (Fig. 2B; 27°C, 0.5 ± 0.4 pA/pF, n = 6; 27°C + butyrate (But), 2.0 ± 1.1 pA/pF, n = 15). In total, our results with the RKR/AAA as well as R15A/K16A and R15A/R17A channels demonstrate that the lack of functional expression cannot be explained by an inability of these mutated channels to traffic to the cell surface.

Increasing Ca^{2+} activates RKR/AAA-expressing hIK1 channels. We demonstrate that expression of the RKR/AAA mutation results in a dramatically reduced DCEBIO-stimulated, clotrimazole-inhibited current density compared to wild-type channels (Fig. 1B and C). This altered response could be caused by (a) an inability of the channel to respond to DCEBIO, (b) an inability of the channel to respond to Ca^{2+} and hence DCEBIO (DCEBIO activation requires Ca^{2+};[1,28,29]) or (c) another regulator of channel function is dependent upon this RKR domain. To begin to evaluate the Ca^{2+} dependence of the RKR/AAA expressing channels we stimulated the cells with the Ca^{2+} ionophore, ionomycin during whole-cell patch-clamp recordings.

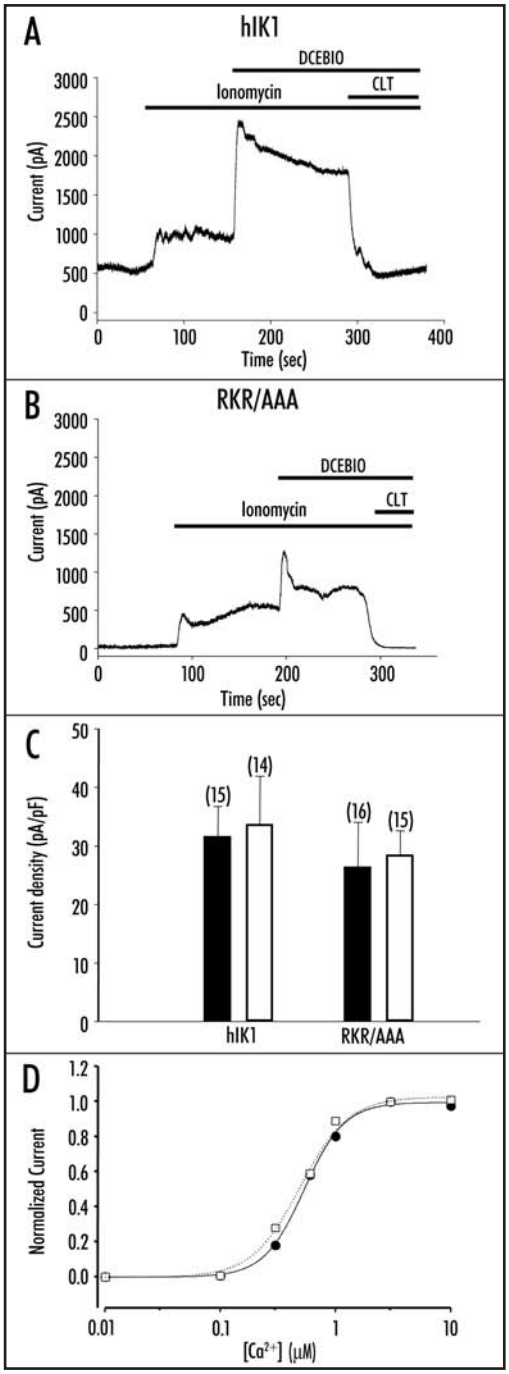

Figure 3. Increased Ca^{2+} activates RKR/AAA-expressing channels. Representative whole-cell current traces from (A) HA-hIK1 or (B) RKR/AAA stably transfected HEK293 in response to 2 µM ionomycin, 10 µM DCEBIO and 3 µM clotrimazole. (C) Summary bar graph showing that ionomycin (2 µM) increases current density in both wild-type (HA-hIK1) and RKR/AAA-expressing cells (solid bars). Subsequent to ionomycin, DCEBIO (10 µM) induces an equivalent increase in current density in wild-type and RKR/AAA-expressing cells (open bars). The numbers of experiments are indicated in parenthesis. The values are not statistically different between HA-hIK1 and RKR/AAA-expressing cells. (D) Average Ca^{2+} concentration-response curves for wild-type hIK1 (filled circles, solid line, n = 12) and RKR/AAA-expressing (open squares, dashed line, n = 11) cells. Error bars have been omitted for clarity. The lines show the best fit to the data using Hill equation ($I = [Ca^{2+}]^n/(K_{0.5}{}^n + [Ca^{2+}]^n)$). The apparent affinity ($K_{0.5}$) and Hill coefficient were not different for wild-type and RKR/AAA hIK1 (WT, $K_{0.5}$ = 512 ± 7nM, Hill coefficient = 2.7; RKR/AAA, $K_{0.5}$ = 527 ± 29 nM, Hill coefficient = 2.7).

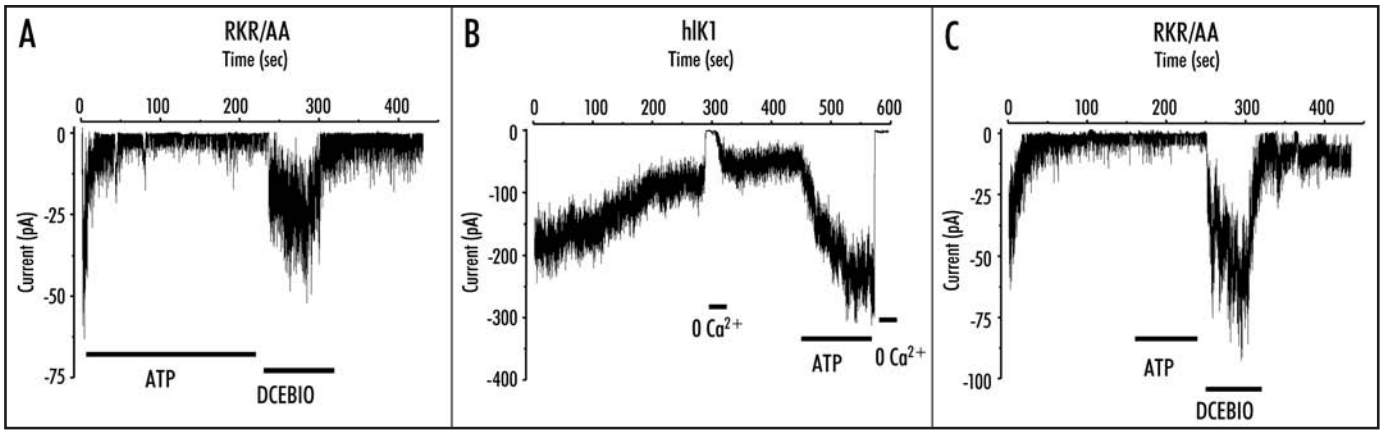

Figure 4. ATP fails to activate RKR/AAA-expressing hIK1 channels. (A) Following patch excision into 10 μM free Ca^{2+} plus 1 mM ATP, RKR/AAA-expressing channels exhibit a rapid decrease in current, so-called "rundown." Subsequent addition of DCEBIO (10 μM) increases current which is reversed upon washout. (B) Following patch excision into 10 μM free Ca^{2+}, in the absence of ATP, wild-type hIK1 channels exhibit a slow rundown. Removal of Ca^{2+} from the bath results in an immediate inhibition of channel activity, which is restored upon re-addition of Ca^{2+}. The subsequent addition of ATP (1 mM) results in a large increase in channel activity, which is completely inhibited by returning to zero Ca^{2+}. (C) Excising RKR/AAA-expressing channels into 10 μM free Ca^{2+}, in the absence of ATP, results in a rapid rundown of channel activity. Addition of ATP (1 mM) does not increase channel activity, although the subsequent addition of DCEBIO (10 μM) results in a large increase in channel activity, which is reversed following washout of DCEBIO.

Figure 3A shows the whole-cell current response to ionomycin (2 μM) for a wild-type hIK1 transfected cell. Ionomycin induced a sustained increase in whole-cell current, which was further increased by the addition of DCEBIO (10 μM). Likewise, in the RKR/AAA expressing channels ionomycin induced a sustained current response, which was further augmented by DCEBIO (Fig. 3B). In both wild-type and RKR/AAA-expressing cells DCEBIO induced an initial transient increase in current followed by a sustained plateau. Ionomycin (2 μM) increased the current densities of wild-type and RKR/AAA to a similar extent (Fig. 3C, filled bars; WT, 31.4 ± 5.3 pA/pF, n = 15; RKR/AAA, 26.2 ± 7.9 pA/pF, n = 16). Importantly, after stimulating with ionomycin, DCEBIO (10 μM) induced a similar additional increase in the steady-state current density in both wild-type- and RKR/AAA-expressing cells (Fig. 3C, open bars; WT, 33.4 ± 8.4 pA/pF, n = 14; RKR/AAA, 28.2 ± 4.4 pA/pF, n = 15). These results clearly demonstrate that the RKR/AAA-expressing hIK1 channels are capable of responding to both Ca^{2+} and DCEBIO.

The apparent Ca^{2+} affinity of hIK1 is not altered by the RKR/AAA mutation. While the above results demonstrate that increasing levels of Ca^{2+} activate the RKR/AAA-expressing channels it is important to determine whether there is an altered apparent Ca^{2+} affinity induced by this mutation. For these studies, we utilized the inside-out patch-clamp technique and, following rundown of the channels to a new steady-state, exposed the patch to increasing levels of Ca^{2+}. These data were then fit to the Hill equation to determine the half-maximal Ca^{2+} concentration ($K_{0.5}$) and Hill coefficient for Ca^{2+}-dependent activation. As shown in Figure 3D, the apparent $K_{0.5}$ and Hill coefficient for Ca^{2+} was not different between wild-type ($K_{0.5}$ = 512 ± 7 nM, Hill coefficient = 2.7 ± 0.3; n = 12) and RKR/AAA-expressing ($K_{0.5}$ = 527 ± 29 nM, Hill coefficient = 2.7 ± 0.3; n = 11) channels, indicating this mutation does not alter the Ca^{2+}-dependent gating of hIK1.

The RKR/AAA mutation abolishes the ATP-dependent activation of hIK1. During the course of our studies designed to elucidate the Ca^{2+}-dependence of hIK1 activation we observed a rundown of the RKR/AAA channel activity, despite the continued presence of ATP (300 μM), following patch excision. It should be noted that this rundown is highly variable (compare Figs. 4A, 6B and 8C). As we have previously shown that this rundown can be precluded by the addition of ATP in a Mg^{2+}-dependent fashion, we have hypothesized that this is due to the existence of a protein phosphatase in the patch.[10] Based on the variability of this response we have not made any attempt to quantify this rate of current decline. This rundown, in the continued presence of ATP, is illustrated in Figure 4A for a single patch excised into saturating levels of Ca^{2+} (10 μM). In five patches the current averaged -13.3 ± 4.9 pA immediately following patch excision and this ran down to -1.5 ± 0.5 pA in the continued presence of ATP. Consistent with our whole-cell patch-clamp recordings, in the presence of high Ca^{2+} (10 μM), DCEBIO (10 μM) increased the mean current to -18.5 ± 9.8 pA. These results confirm our whole-cell patch-clamp data by demonstrating that the RKR/AAA mutation does not preclude these channels from responding to the pharmacological opener, DCEBIO. However, we were surprised by the magnitude of the rundown in current observed following patch excision in the presence of ATP. We[10] previously demonstrated that ATP greatly diminishes this rundown and reactivates the channel following rundown in wild-type hIK1 channels. This activation of wild-type hIK1 by ATP is shown for a single recording in Figure 4B. In four patches, ATP increased the mean current an average of 4.1 ± 0.9-fold; similar to the 3.5-fold increase in current we previously reported for hIK1.[9] We next determined whether ATP (1 mM) could reactivate RKR/AAA-expressing channels following rundown, similar to wild-type channels. A representative current trace is shown in Figure 4C. For these experiments the channels were excised into 10 μM Ca^{2+} in the absence of ATP. Following rundown of current, ATP was perfused onto the patch. As is apparent, ATP failed to activate the RKR/AAA-expressing channels, although the subsequent addition of DCEBIO (10 μM) resulted in rapid activation. In eight patches the current averaged -27.0 ± 2.6 pA immediately following patch excision and this decreased to -9.0 ± 4.6 pA in the continued presence of 10 μM Ca^{2+}. The subsequent addition of ATP (1 mM) failed to increase channel activity (-7.5 ± 4.7 pA), whereas DCEBIO (10 μM) dramatically increased mean current to -75.4 ± 33.6 pA. These results demonstrate that the NH_2-terminal RKR domain is required for the ATP-dependent activation of hIK1. As ATP

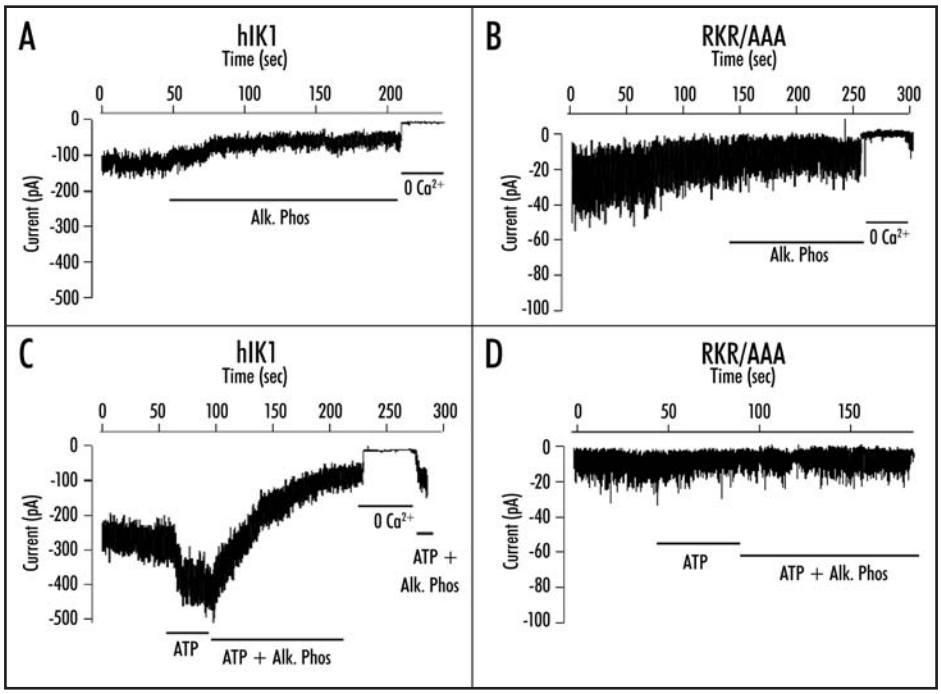

Figure 5. Patches from HEK293 cells stably transfected with either HA-hIK1 (A and C) or RKR/AAA (B and D) are excised into a bath containing 10 μM free Ca^{2+}. Note that the recordings shown in this figure were initiated subsequent to the rundown of channel activity. (A) Following the establishment of a steady-state current wild-type hIK1 channel activity was further decreased in the presence of alkaline phosphatase (5 U/ml). (B) Alkaline phosphatase (5 U/ml) has no effect on RKR/AAA channels, although 0 Ca^{2+} eliminates channel activity. (C) Wild-type hIK1 channels are activated by ATP (1 mM) in the presence of saturating Ca^{2+} and this effect is reversed by the subsequent addition of alkaline phosphatase (10 U/ml) in the continued presence of ATP. (D) RKR/AAA-expressing channels are not activated by ATP (1 mM) and the subsequent addition of alkaline phosphatase (10 U/ml) has no effect on channel activity.

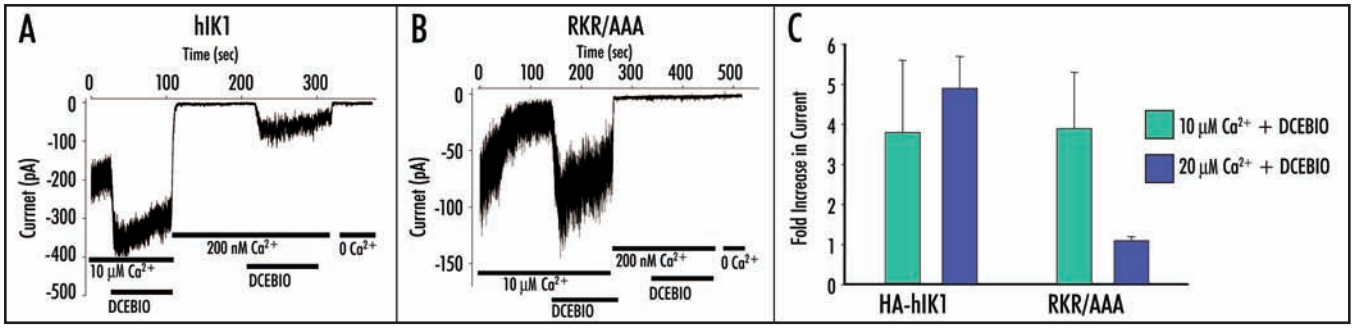

Figure 6. Patches from HEK293 cells stably transfected with either (A) HA-hIK1 or (B) RKR/AAA cells are excised into a bath containing 10 μM free Ca^{2+}. The channels are further activated with 10 μM DCEBIO. The bath is then switched to 200 nM Ca^{2+} and subsequently exposed to 10 μM DCEBIO. (B) The RKR/AAA channels cannot reactivate at low Ca^{2+}. (C) DCEBIO-stimulated increase in current for wild-type (n = 17) and RKR/AAA (n = 7) hIK1 in the presence of either 10 μM (blue bars) or 200 nM (green bars) free Ca^{2+}.

is known to alter the Ca^{2+}-dependent gating of hIK1[9] this likely explains the difference observed between our whole-cell recordings (100 nM free Ca^{2+}) and our excised patch-clamp recordings (10 μM free Ca^{2+}; see Discussion).

The RKR/AAA mutation abolishes the alkaline phosphatase-dependent inhibition of hIK1. The above results suggest that the RKR/AAA mutation eliminates the kinase-dependent regulation of hIK1 which we previously described,[9,10] resulting in a channel with a marked reduction in P_o. As we previously demonstrated that this ATP-dependent activation of hIK1 could be reversed by alkaline phosphatase, indicative of a kinase-mediated event,[10] our present results would predict that the RKR/AAA-expressing channels would be insensitive to alkaline phosphatase. Initially we confirmed the alkaline phosphatase-dependence of wild-type hIK1. As shown in Figure 5A, following patch excision in the absence of ATP and the establishment of a steady-state current, wild-type hIK1 activity was further decreased by the addition of alkaline phosphatase (5 U/ml). In seven experiments, the steady-state current averaged 118 ± 19 pA which was reduced to 53 ± 14 pA following addition of alkaline phosphatase. In a separate series of experiments (Fig. 5C), channel activity was increased by the addition of ATP (1 mM). The subsequent addition of alkaline phosphatase (10 U/ml) again dramatically reduced this current. In six experiments the steady-state current averaged 113 ± 34 pA and this was increased to 146 ± 50 pA by the addition of

ATP. Further addition of alkaline phosphatase (10 U/ml) reduced this current to 44 ± 9 pA, similar to what we previously reported.[10]

In contrast to the above results, following rundown of the RKR/AAA-expressing channels the current was not increased by ATP and was not inhibited by alkaline phosphatase (Fig. 5B and D). In five experiments the current averaged 19 ± 3 pA and this was not altered by alkaline phosphatase (5 U/ml; 18 ± 2 pA). In an additional five experiments the current was not increased by ATP (control, 11 ± 2 pA; ATP, 11 ± 2 pA) nor reduced by the subsequent addition of alkaline phosphatase (10 U/ml; 11 ± 2 pA). These results clearly demonstrate that the RKR/AAA mutation eliminates the ATP- and alkaline phosphatase-dependent regulation of hIK1.

The activation of RKR/AAA by DCEBIO is Ca^{2+} dependent. We demonstrate that wild-type hIK1 expressing cells respond to DCEBIO in the presence of both low levels of intracellular Ca^{2+} (200 nM, Fig. 1) as well as in the presence of elevated Ca^{2+} (ionomycin stimulated, Fig. 3). In contrast, RKR/AAA-expressing cells only respond to DCEBIO in the presence of elevated Ca^{2+} (ionomycin, Figs. 1 and 3) during whole-cell recording. To extend these observations, we utilized the inside-out patch-clamp technique where the DCEBIO dependence on Ca^{2+} levels can be more directly evaluated in wild-type- and RKR/AAA-expressing cells. As shown in Figure 6A, excising wild-type hIK1 into saturating Ca^{2+} (10 μM) results in actively gating channels, which can be further activated by DCEBIO, as previously reported.[29] This activation averaged 3.8 ± 1.8-fold in 17 patches. Following reduction in bath Ca^{2+} to 200 nM channel activity was significantly decreased. Once more, the addition of DCEBIO resulted in a large increase in channel activity, averaging 4.9 ± 0.8-fold (n = 17). As shown in Figure 6B, DCEBIO similarly activated RKR/AAA in the presence of saturating Ca^{2+} (10 μM), averaging 3.9 ± 1.4-fold in seven patches. However, following reduction of free Ca^{2+} to 200 nM, DCEBIO failed to increase RKR/AAA channel activity (1.1 ± 0.1-fold, n = 7). These results are consistent with our whole-cell data and demonstrate that the activation of RKR/AAA by DCEBIO is dependent upon elevated Ca^{2+}.

The activation of hIK1 by DCEBIO is ATP dependent. We demonstrate: (a) ATP fails to activate RKR/AAA (Fig. 4); (b) alkaline phosphatase does not alter RKR/AAA function (Fig. 5), suggesting that RKR/AAA-expressing channels are not phosphorylated; and (c) that the activation of RKR/AAA by DCEBIO is dependent upon the level of free Ca^{2+} in the bath (Fig. 6). This raises the question of whether these observations are directly linked. That is, we have previously shown that ATP activates hIK1 by increasing the channel open probability (P_o) at all levels of Ca^{2+} while not shifting apparent Ca^{2+} affinity.[10] Here we demonstrate that RKR/AAA fails to respond to ATP, i.e., it is behaving in a manner analogous to hIK1, which has not been exposed to ATP. Thus, RKR/AAA-expressing channels would have a lower P_o at all levels of Ca^{2+} than wild-type hIK1 in the presence of ATP. We previously demonstrated that the activation of hIK1 by EBIO is dependent upon the channel being actively gating in the presence of Ca^{2+}, i.e., EBIO can not activate hIK1 in the absence of Ca^{2+}.[1] Thus, we would propose that following de-phosphorylation, hIK1 would have a reduced response to DCEBIO, analogous to the RKR/AAA channels. To test this hypothesis we determined the effect of alkaline phosphatase (5 U/ml) on hIK1 channel activity in the presence of DCEBIO. As shown in Figure 7, decreasing free Ca^{2+} from 10 μM to 200 nM resulted in a large decrease in channel activity which was stimulated 4.8 ± 1.4-fold by DCEBIO. The subsequent addition of alkaline phosphatase reduced channel activity

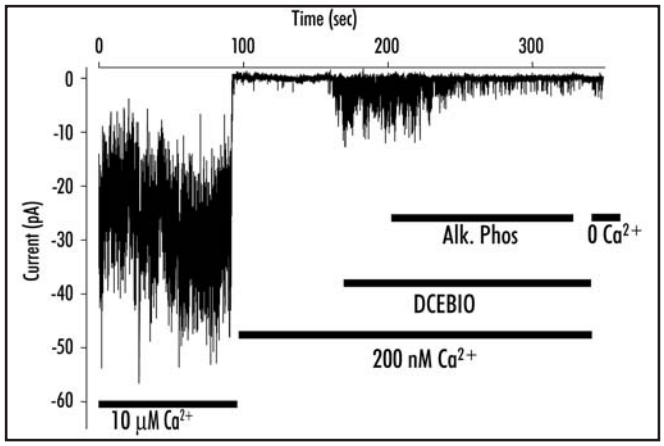

Figure 7. Alkaline phosphatase inhibits hIK1 response to DCEBIO. The patch is excised from a wild-type HA-hIK1 expressing HEK cell into a bath containing 10 μM free Ca^{2+}. The subsequent reduction in free Ca^{2+} to 200 nM decreased current, and this activity could be increased with the addition of DCEBIO (10 μM). The further addition of alkaline phosphatase (5 U/ml) results in a loss of channel activity (n = 9).

such that the response above baseline was only 1.3 ± 0.6 fold (n = 9). This result is consistent with the notion that the RKR/AAA channels are analogous to a de-phosphorylated wild-type hIK1 channel such that their P_o is dramatically reduced. This reduced P_o results in a channel, which cannot respond to DCEBIO, as we have previously reported for wild-type hIK1 in the absence of Ca^{2+}.

RKR/AAA channels have a reduced P_o compared to wild-type hIK1. The above results suggest that the RKR/AAA channels will have a reduced P_o compared to wild-type hIK1. Unfortunately, patches expressing wild-type hIK1, where the number of individual channels can be accurately determined are rarely observed in our cell line and so standard methods of estimating channel P_o cannot be utilized. Thus, we used variance analysis to estimate channel P_o as the channel was activated first with ATP and then DCEBIO (see Methods). A representative experiment for wild-type hIK1 is shown in Figure 8A. Following patch excision into 10 μM Ca^{2+}, in the absence of ATP, channel activity decreased over time until it reached a steady state. Addition of ATP (300 μM) increased channel activity as previously described,[9,10] and this was further increased by DCEBIO. The variance plot for this channel recording is shown in Figure 8B. As is apparent, the variance goes through a maximum such that the maximum P_o (P_{oMAX}) for this recording is 0.64 in the presence of DCEBIO. In 6 patches the P_{oMAX} in the presence of DCEBIO averaged 0.69 ± 0.02, with a single channel amplitude of 2.1 ± 0.1 pA. Based on this P_{oMAX}, we are able to calculate a P_o in the presence of 10 μM Ca^{2+} and ATP of 0.38 ± 0.03 and a P_o in the presence of only 10 μM $Ca^{2+}$of 0.10 ± 0.06.

In contrast to wild-type hIK1, ATP did not induce a significant increase in current in RKR/AAA, in the presence of 10 μM Ca^{2+}, whereas DCEBIO stimulated a large response (Fig. 8C). An analysis of variance for this recording demonstrates a P_{oMAX} of 0.61 (Fig. 8D). In four patches, the P_{oMAX} for RKR/AAA averaged 0.63 ± 0.05, which is not significantly different from wild-type hIK1. However, based on these measurements, the calculated P_o for RKR/AAA in the presence of 10 μM Ca^{2+} and ATP is only 0.11 ± 0.03, a value significantly less than wild-type hIK1 ($p < 0.001$). This value is not different from that in the presence of 10 μM Ca^{2+} alone (P_o = 0.09 ± 0.02). Indeed, this value is the same as that predicted for wild-type hIK1 in the

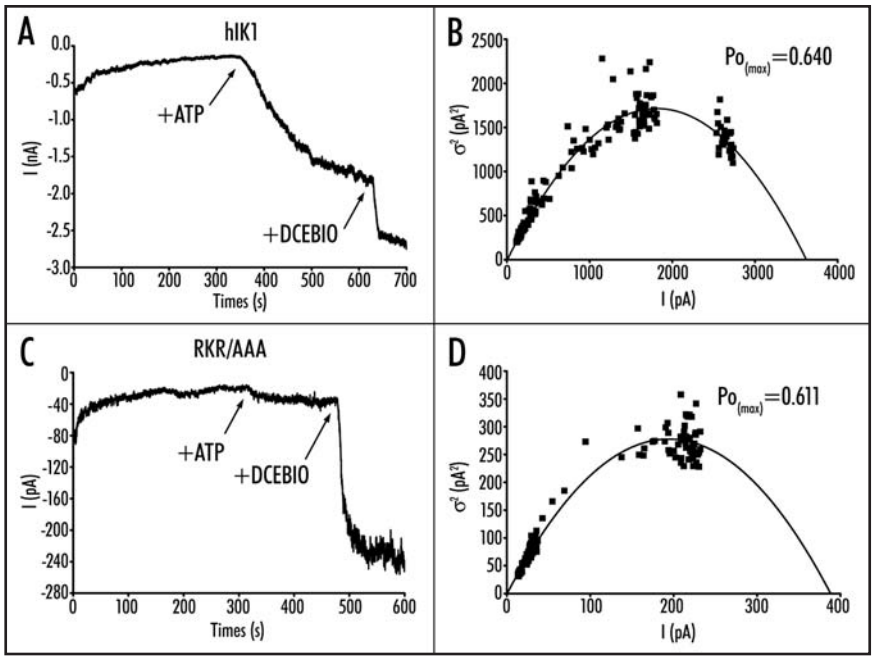

Figure 8. Variance analysis of wild-type and RKR/AAA hIK1. (A) Following patch excision of wild-type hIK1 into a bath containing 10 μM free Ca^{2+} current decreased over time until a new steady-state was reached. The subsequent addition of both ATP (1 mM) and DCEBIO (10 μM) resulted in an increase in current flow. Current traces have been data reduced for display. Spike artifacts during solution changes were removed prior to analysis as they produce large deviations during variance analysis. (B) Plot of variance (σ^2) against mean current (I) for the current record shown in (A). The data were fitted to equation 1 yielding an N of 1,907 ± 45 channels and a single channel amplitude (i) of 1.90 ± 0.03 pA. These data allowed us to calculate a P_{oMAX} of 0.64 for this recording using equation 2. (C) Excised patch-clamp recording of RKR/AAA hIK1 demonstrating a loss of ATP-dependent activation. (D) Plot of variance (σ^2) against mean current (I) for the current record shown in (C). The data were fitted to equation 1 yielding an N of 136 ± 5 channels and a single channel amplitude (i) of 2.87 ± 0.05 pA. These data allowed us to calculate a P_{oMAX} of 0.61 for this recording using equation 2.

absence of ATP (0.10 ± 0.06), further suggesting that the RKR/AAA mutation behaves similarly to wild-type hIK1, which has not been exposed to ATP.

We were able to obtain three patches on RKR/AAA where we could accurately count the number of channels in the presence of DCEBIO and thus directly estimate P_o. Figure 9 shows the results from one patch containing 12 channels. In the absence of DCEBIO only three channel levels were observed both in the channel record (Fig. 9A) and the amplitude histogram (Fig. 9B). Following DCEBIO addition (10 μM), channel activity was dramatically increased and 12 channel levels could be discerned in the amplitude histogram. The dashed line shows the fits to the individual peaks in the amplitude histogram while the colored lines show the sum of these individual peaks for ATP (red) and DCEBIO (blue). We are confident that we are not underestimating the number of channels in the patch (n) as each individual level probability (P_i) is in excellent agreement with a binomial distribution (see Equation 5). Based on these data, we calculate a P_o in the absence of DCEBIO (in the presence of ATP) of 0.036, which is increased to 0.603 in the presence of DCEBIO. In four patches the average P_o increased from 0.044 ± 0.004 in the å

DISCUSSION

While the NH_2-terminus of hIK1 is predicted to be only 26 amino acids long it contains numerous well-defined motifs, including a leucine zipper, di-leucine and multi-basic motifs, known to play crucial roles in the assembly, regulation and trafficking of a host of proteins. Indeed, we recently defined a role for both the NH_2-terminal leucine zipper and di-leucine motifs in the assembly and trafficking of hIK1.[14] While hIK1 possesses a cytoplasmic NH_2-terminal multi-basic motif (RRRKR) closely apposed to the predicted first transmembrane domain,[30,31] the role of this domain has not previously been evaluated. Multi-basic motifs are known to play crucial roles in a wide array of cell biological processes, including ER exit,[17,32] ER retention,[15,16] acting as nuclear localization signals[33,34] as well as the gating of K^+ channels.[18,19] Thus, the role these multi-basic motifs play in protein trafficking and function is dependent upon the context in which they are expressed. Here we demonstrate that the ATP-dependent activation and alkaline phosphatase-dependent inhibition of hIK1 is dependent upon a multi-basic RKR motif. That is, mutating this motif results in a channel with a dramatically reduced P_o such that it behaves like wild-type hIK1, which has not been exposed to ATP. As we have previously demonstrated a role for the C-terminus in the ATP-dependent activation of hIK1, our results are consistent with the hypothesis that the ATP-dependent regulation of hIK1 is conferred by the expected close apposition of the NH_2- and C-termini, similar to what has been described for the SK channels.[35]

We initially demonstrate that double and triple mutations of the ^{15}RKR^{17} domain of hIK1 result in a near complete loss of channel activity, as assessed by DCEBIO-induced, clotrimazole-sensitive whole-cell current density measurements (Fig. 1C). We further demonstrate that mutation of the two arginines preceding this RKR motif (R13A/R14A) has no effect on channel function (Fig. 1) suggesting these additional basic amino acids are not part of the motif identified. The lack of a functional response to DCEBIO in these experiments could be the result of several possibilities: First, mutation of this RKR domain could result in the expression of a

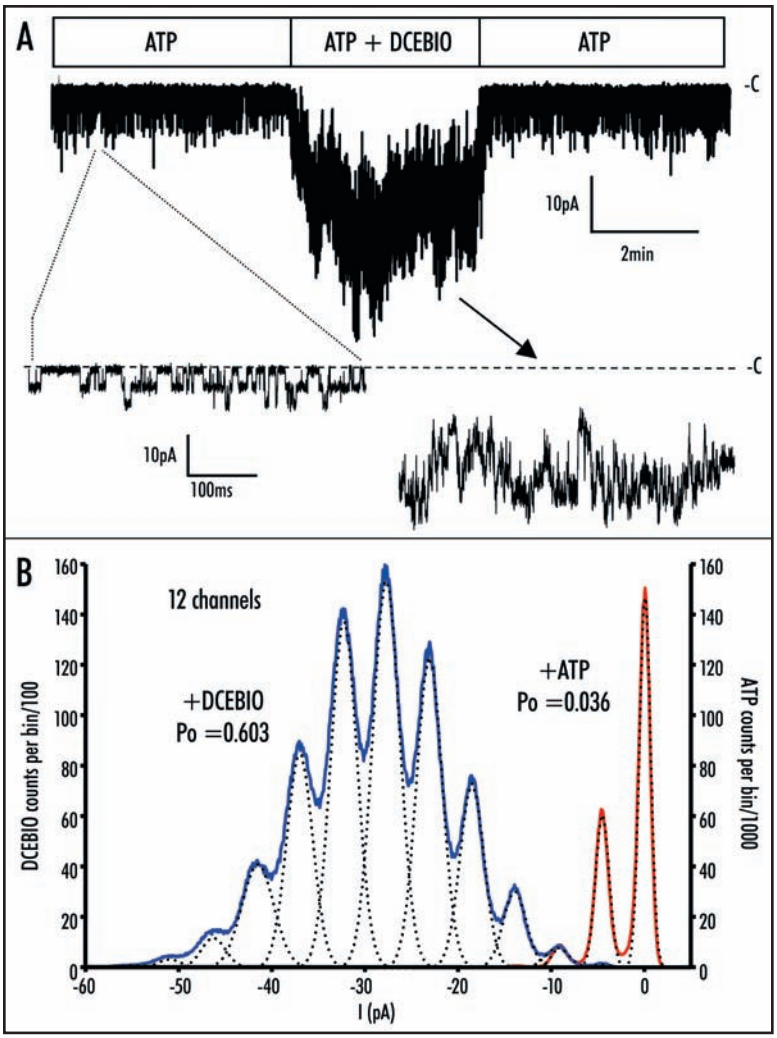

Figure 9. (A) Excised patch of RKR/AAA hIK1 showing activation by DCEBIO (10 μM). Expanded current traces in the presence of ATP (300 μM) and DCEBIO are shown where the dashed line indicates the closed state (-C) of the channel. Changes in seal resistance were compensated for and removed by processing current trace with Biopatch software. Current spike artifacts during solution change have been removed. (B) Amplitude histogram of the recording shown in (A). A bin size of 0.1 pA was used and the data were fit as described in the Methods. The red trace shows the gaussian fit to the current in the presence of ATP, whereas the blue trace shows the gaussian fit to the current trace in the presence of DCEBIO. The dashed lines are the fits to the individual peaks in the amplitude histogram. Based on these fits we calculated open probabilities (P_o) of 0.036 and 0.603 for RKR/AAA hIK1 in the presence of ATP and DCEBIO, respectively.

trafficking defective channel such that the channel fails to express at the cell surface. However, as shown in Figure 1D, the R15A/R17A and R15A/K16A channels were expressed at the cell surface at wild-type levels, although no response to DCEBIO was observed. Additionally, the 4.7-fold decrease in cell surface channel expression, as assessed by cell surface IP, can not account for the 30-fold decrease in current response observed for the RKR/AAA-expressing cells. Finally, while the RKR/AAA mutation resulted in both diminished protein expression as well as cell surface expression this was completely restored by incubating the RKR/AAA expressing channels at 27°C in either the presence or absence of butyrate (Fig. 2A). Despite this increased cell surface expression, the RKR/AAA-expressing channels failed to respond to DCEBIO during whole-cell patch-clamp recording (Fig. 2B). Together, these results indicate that the lack of a functional DCEBIO response during these whole-cell recordings is not the result of altered channel trafficking or expression. Nevertheless, we cannot completely exclude the possibility that the decreased expression observed for the RKR/AAA mutation may in some way alter channel function.

A more likely scenario to explain the lack of a DCEBIO response, despite cell surface expression, is that these NH_2-terminal basic amino acids are necessary for the correct gating of hIK1. This could come about in at least three ways: First, the channels, although trafficking to the plasma membrane, may be functionally dead and therefore incapable of carrying current. However, we demonstrate in both whole-cell (Fig. 3) and excised patch-clamp (Figs. 3, 5 and 6) recordings that the RKR/AAA-expressing channels respond to changes in Ca^{2+}, indicative of an actively gating channel. Second, although the Ca^{2+}-dependent gating of these channels is conveyed via the binding of Ca^{2+} to calmodulin,[36,37] the NH_2-terminus may modify this Ca^{2+}-dependent gating. This hypothesis is refuted by our demonstration that the apparent $K_{0.5}$ and Hill coefficient for Ca^{2+}-dependent gating are not different between wild-type and RKR/AAA-expressing channels (Fig. 3D).

Third, as shown in Figures 4 and 8, the dramatically reduced gating potential of RKR/AAA-expressing hIK1 channels is the result of an inability of these channels to correctly respond to ATP. This result raises the question of why a lack of an ATP response results in a channel which cannot respond to DCEBIO at low Ca^{2+} concentrations (Figs. 1 and 6), but which does respond to DCEBIO at high levels of Ca^{2+} (Figs. 3, 4, 6 and 8)? We previously demonstrated that (a) hIK1 exists in a phosphorylated state following patch excision, (b) the open probability (P_o) of hIK1 could be reduced approximately 50% by exogenous phosphatases, and (c) ATP activates hIK1 via a kinase-dependent mechanism.[9,10] This ATP-dependent activation of hIK1 involved an increase in P_o at all levels of Ca^{2+} with no change in the apparent $K_{0.5}$ or Hill coefficient for Ca^{2+} activation.[10] Here, we demonstrate that the RKR/AAA mutation has no effect on the Ca^{2+}-dependence of channel gating (Fig. 3D). Thus, we interpret our data to indicate that the RKR/AAA mutation is functionally equivalent to a de-phosphorylated channel, i.e., current is dramatically reduced with no change in Ca^{2+}-dependent gating. We, therefore, propose that the inability of the RKR/AAA channels to respond to DCEBIO during our whole-cell patch-clamp experiments is based upon the extremely low P_o expected for hIK1 in 200 nM free Ca^{2+} (pipette solution) in a de-phosphorylated (non-ATP) state. As Ca^{2+}-mediated channel activity is a prerequisite for activation by EBIO[1,28,29] the compromised response to ATP would be expected to impinge upon the DCEBIO-dependent activation at these resting levels of Ca^{2+}. This proposal is supported by a series of experiments. First, while wild-type hIK1 is activated by DCEBIO to a similar extent (3.8 ± 1.8 vs. 4.9 ± 0.8-fold) in both low and high Ca^{2+} (Fig. 6) the response of the RKR/AAA mutation to DCEBIO is completely abrogated in low Ca^{2+} as channel activity is dramatically diminished at these levels of Ca^{2+}. It is important to note that the response of the RKR/AAA mutation to DCEBIO in high Ca^{2+} is identical to wild-type hIK1 (3.8 ± 1.8 vs. 3.9 ± 1.4-fold) indicating the response to DCEBIO is not compromised per se, but that the lack of response in low Ca^{2+} is due to the diminished

channel activity exhibited by the RKR/AAA mutation. Second, if the RKR/AAA mutation behaves as a de-phosphorylated channel then the response to DCEBIO on a wild-type channel should be reduced following the addition of alkaline phosphatase as this would mimic the RKR/AAA mutation. This is exactly what was observed (Fig. 7) and clearly demonstrates that reducing the P_o of hIK1 via a de-phosphorylation mechanism will diminish the ability of DCEBIO to activate the channel. Finally, we utilized variance analysis to measure channel P_o in 10 μM Ca^{2+}, 10 μM Ca^{2+} plus ATP and 10 μM Ca^{2+} plus ATP and DCEBIO. We demonstrate that wild-type hIK1 has an P_o in 10 μM Ca^{2+} alone that is identical to the P_o of RKR/AAA in the presence of 10 μM Ca^{2+} plus ATP (0.10 vs. 0.11, respectively). We confirmed this low P_o for RKR/AAA directly in excised patches expressing relatively low numbers of channels (P_o = 0.044), demonstrating the utility of the variance analysis approach. Given the very low P_o of RKR/AAA in saturating Ca^{2+} (P_o = 0.04 to 0.1) this mutation would result in a completely inactive channel at resting levels of Ca^{2+}, thus explaining the lack of response to DCEBIO in 200 nM free Ca^{2+} (Figs. 1 and 6). Given the observations that (a) RKR/AAA has a P_o in the presence of 10 μM Ca^{2+} plus ATP that is identical to wild-type hIK1 in 10 μM Ca^{2+} alone, (b) that RKR/AAA fails to respond to ATP or alkaline phosphatase and (c) the effect of the RKR/AAA mutation can be mimicked by de-phosphorylating wild-type hIK1 we conclude that the multi-basic RKR motif is required for ATP-dependent activation of hIK1.

It is interesting to note that Hirschberg et al.[38] observed an P_o of approximately 0.6 for SK2 channels in saturating Ca^{2+} (note however, that transitions to a low P_o were spontaneously observed), whereas we observe a P_o of only approximately 0.1 for hIK1 in saturating Ca^{2+} in the absence of additional modulators of channel activity. As Ca^{2+} is known to primarily alter the channel opening rate,[38] this would suggest that while IK and SK channels are highly conserved throughout the pore and calmodulin binding domains the energetics involved in the Ca^{2+}-dependent transition between the closed and open states are markedly different. We also consistently observe a decrease in current flow across the patch following excision from the cell (present data and refs. 9 and 10), suggesting that hIK1 (or an alternate protein that modulates hIK1 function) is phosphorylated cell-attached. Indeed, in the phosphorylated state, hIK1 has an P_o approaching that of the SK channels. Also, while the crystal structure for the calcified and apo-calmodulin-bound calmodulin-binding domains have been solved,[39,40] the mechanism whereby this results in channel opening, how this is distinct between hIK1 and rSK2 and how ATP influences this transition remain unclear.

It is also critical to note that the RKR/AAA mutation does not abrogate rundown of the channel following patch excision (Figs. 4, 6 and 8), although the ATP-dependent activation and alkaline phosphatase-dependent inhibition are lost (Figs. 4, 5 and 8). Thus, we must consider the possibility that there are two distinct regulatory events being observed in these recordings. First, there is rundown of the channel and second there is an ATP-dependent activation, which we have previously shown to be kinase driven.[9,10] One possibility to explain the ATP-independent run-down observed in the RKR/AAA mutation (Figs. 4, 6 and 8), is that this is dependent upon lipid mediators, such as PIP_2. PIP_2 is a well-known modulator of channel function[41,42] and has been shown to depend upon positively charged amino acids in cytosolic domains.[43-45] However, we (unpublished observations) and Donald Hilgemann (personal communication) have found no effect of PIP_2 on hIK1 channel function. Similarly, we found no effect of PI(3)P on hIK1 function in inside-out patches (unpublished observations). Thus, these lipid mediators cannot explain the rundown observed in hIK1 that is ATP-independent.

It is important to note that we previously reported that the ATP-dependent activation of hIK1 was dependent upon a 14 amino acid region within the Ca^{2+}-dependent calmodulin-binding domain of the C-terminus.[9] As this region of hIK1 contains no consensus phosphorylation sites, we speculated that a β-subunit might be involved in the ATP-dependent regulation observed. Our present results clearly demonstrate that the NH_2-terminus of hIK1 is involved in the ATP-dependent activation of hIK1. Based on these results, we would modify our hypothesis to suggest that the ATP-dependent activation of hIK1 involves a close association between the NH_2- and C-termini of the channel, although further experimentation is required to directly address this possibility.

In this regard, Skolnik and colleagues[46] identified a novel β-subunit of hIK1, MTMR6, which belongs to a family of phosphatases that dephosphorylate the 3' position of phosphatidylinositol 3-phosphate (PI(3)P). Interestingly, MTMR6 was shown to interact with hIK1 via a C-terminal leucine zipper,[47] which we previously demonstrated was required for the correct trafficking of hIK1 to the cell surface.[13] Further, the MTMR6-dependent regulation of hIK1 requires the identical 14 amino acid C-terminal domain[47] that we mapped as being critical for the ATP-dependent activation of hIK1.[9] More recently, these authors demonstrated that nucleoside diphosphate kinase B (NDK-B) functions downstream of PI(3)P to directly phosphorylate a histidine in this 14 amino acid C-terminal domain.[48] Thus, the ATP-dependent regulation of hIK1 which we initially demonstrated[9,10] may be due to the NDK-B model described by Skolnik and colleagues.[48] How the RKR domain described in the present work may impinge upon this novel regulatory mechanism remains to be determined.

In conclusion, we demonstrate that mutation of an NH_2-terminal RKR domain in hIK1 results in a complete loss of ATP-dependent activation. This results in a channel with a reduced P_o such that the response to pharmacologic agents is also compromised; further highlighting the relationship between Ca^{2+}, kinase (ATP) and pharmacologic (DCEBIO) activators of hIK1. These results represent the first demonstration for a role of the NH_2-terminus in the second messenger-dependent regulation of hIK1.

References

1. Devor DC, Singh AK, Frizzell RA, Bridges RJ. Modulation of Cl- secretion by benzimidazolones. I. Direct activation of a Ca^{2+}-dependent K^+ channel. Am J Physiol 1996; 271:L775-84.
2. Devor DC, Singh AK, Lambert LC, DeLuca A, Frizzell RA, Bridges RJ. Bicarbonate and chloride secretion in Calu-3 human airway epithelial cells. J Gen Physiol 1999; 113:743-60.
3. Edwards G, Gardener MJ, Feletou M, Brady G, Vanhoutte PM, Weston AH. Further investigation of endothelium-derived hyperpolarizing factor (EDHF) in rat hepatic artery: Studies using 1-EBIO and ouabain. Br J Pharmacol 1999; 128:1064-70.
4. Ghanshani S, Wulff H, Miller MJ, Rohm H, Neben A, Gutman GA, Cahalan MD, Chandy KG. Up-regulation of the IKCa1 potassium channel during T-cell activation: Molecular mechanism and functional consequences. J Biol Chem 2000; 275:37137-49.
5. Kohler R, Degenhardt C, Kuhn M, Runkel N, Paul M, Hoyer J. Expression and function of endothelial Ca^{2+}-activated K^+ channels in human mesenteric artery: A single-cell reverse transcriptase-polymerase chain reaction and electrophysiological study in situ. Circ Res 2000; 87:496-503.
6. Vandorpe DH, Shmukler BE, Jiang L, Lim B, Maylie J, Adelman JP, de Franceschi L, Cappellini MD, Brugnara C, Alper SL. cDNA cloning and functional characterization of the mouse Ca^{2+}-gated K^+ channel, *mIK1*: Roles in regulatory volume decrease and erythroid differentiation. J Biol Chem 1998; 273:21542-53.
7. Keen JE, Khawaled R, Farrens DL, Neelands T, Rivard A, Bond CT, Janowsky A, Fakler B, Adelman JP, Maylie J. Domains responsible for constitutive and Ca^{2+}-dependent interactions between calmodulin and small conductance Ca^{2+}-activated potassium channels. J Neurosci 1999; 19:8830-8.

8. Khanna R, Chang MC, Joiner WJ, Kaczmarek LK, Schlichter LC. hSK4/hIK1, a calmodulin-binding KCa channel in human T lymphocytes: Roles in proliferation and volume regulation. J Biol Chem 1999; 274:14838-49.
9. Gerlach AC, Syme CA, Giltinan L, Adelman JP, Devor DC. ATP-dependent activation of the intermediate conductance, Ca^{2+}-activated K^+ channel, hIK1, is conferred by a C-terminal domain. J Biol Chem 2001; 276:10963-70.
10. Gerlach AC, Gangopadhyay NN, Devor DC. Kinase-dependent regulation of the intermediate conductance, calcium-dependent potassium channel, hIK1. J Biol Chem 2000; 275:585-98.
11. Wulf A, Schwab A. Regulation of a calcium-sensitive K^+ channel (cIK1) by protein kinase C. J Membr Biol 2002; 187:71-9.
12. Joiner WJ, Khanna R, Schlichter LC, Kaczmarek LK. Calmodulin regulates assembly and trafficking of SK4/IK1 Ca^{2+}-activated K^+ channels. J Biol Chem 2001; 276:37980-5.
13. Syme CA, Hamilton KL, Jones HM, Gerlach AC, Giltinan L, Papworth GD, Watkins SC, Bradbury NA, Devor DC. Trafficking of the Ca^{2+}-activated K^+ channel, hIK1, is dependent upon a C-terminal leucine zipper. J Biol Chem 2003; 278:8476-86.
14. Jones HM, Hamilton KL, Papworth GD, Syme CA, Watkins SC, Bradbury NA, Devor DC. Role of the NH2 terminus in the assembly and trafficking of the intermediate conductance Ca^{2+}-activated K^+ channel hIK1. J Biol Chem 2004; 279:15531-40.
15. Margeta-Mitrovic M, Mitrovic I, Riley RC, Jan LY, Basbaum AI. Immunohistochemical localization of GABA(B) receptors in the rat central nervous system. J Comp Neurol 1999; 405:299-321.
16. Zerangue N, Schwappach B, Jan YN, Jan LY. A new ER trafficking signal regulates the subunit stoichiometry of plasma membrane K(ATP) channels. Neuron 1999; 22:537-48.
17. Perego C, Bulbarelli A, Longhi R, Caimi M, Villa A, Caplan MJ, Pietrini G. Sorting of two polytopic proteins, the gamma-aminobutyric acid and betaine transporters, in polarized epithelial cells. J Biol Chem 1997; 272:6584-92.
18. Schulte U, Hahn H, Wiesinger H, Ruppersberg JP, Fakler B. pH-dependent gating of ROMK (Kir1.1) channels involves conformational changes in both N and C termini. J Biol Chem 1998; 273:34575-9.
19. Cukras CA, Jeliazkova I, Nichols CG. The role of NH2-terminal positive charges in the activity of inward rectifier KATP channels. J Gen Physiol 2002; 120:437-46.
20. Singh S, Syme CA, Singh AK, Devor DC, Bridges RJ. Benzimidazolone activators of chloride secretion: Potential therapeutics for cystic fibrosis and chronic obstructive pulmonary disease. J Pharmacol Exp Ther 2001; 296:600-11.
21. Alvarez O, Gonzalez C, Latorre. R. Counting channels: A tutorial guide on ion channel fluctuation analysis. Adv Physiol Educ 2002; 26:327-41.
22. Sigworth FJ. Sodium channels in nerve apparently have two conductance states. Nature 1977; 270:265-7.
23. Sigworth FJ. The variance of sodium current fluctuations at the node of Ranvier. Journal of Physiology 1980; 307:97-129.
24. Traynelis SF, Jaramillo F. Getting the most out of noise in the central nervous system. Trends in Neurosciences 1998; 21:137-45.
25. Rubenstein RC, Egan ME, Zeitlin PL. In vitro pharmacologic restoration of CFTR-mediated chloride transport with sodium 4-phenylbutyrate in cystic fibrosis epithelial cells containing delta F508-CFTR. J Clin Invest 1997; 100:2457-65.
26. Denning GM, Anderson MP, Amara JF, Marshall J, Smith AE, Welsh MJ. Processing of mutant cystic fibrosis transmembrane conductance regulator is temperature-sensitive. Nature 1992; 358:761-4.
27. Zhou Z, Gong Q, January CT. Correction of defective protein trafficking of a mutant *HERG* potassium channel in human long QT syndrome: Pharmacological and temperature effects. J Biol Chem 1999; 274:31123-6.
28. Singh AK, Devor DC, Gerlach AC, Gondor M, Pilewski JM, Bridges RJ. Stimulation of Cl(-) secretion by chlorzoxazone. J Pharmacol Exp Ther 2000; 292:778-87.
29. Syme CA, Gerlach AC, Singh AK, Devor DC. Pharmacological activation of cloned intermediate- and small-conductance Ca^{2+}-activated K^+ channels. Am J Physiol Cell Physiol 2000; 278:C570-81.
30. Ishii TM, Silvia C, Hirschberg B, Bond CT, Adelman JP, Maylie J. A human intermediate conductance calcium-activated potassium channel. Proc Natl Acad Sci USA 1997; 94:11651-6.
31. Joiner WJ, Wang LY, Tang MD, Kaczmarek LK. hSK4, a member of a novel subfamily of calcium-activated potassium channels. Proc Natl Acad Sci USA 1997; 94:11013-8.
32. Keller SH, Lindstrom J, Ellisman M, Taylor P. Adjacent basic amino acid residues recognized by the COP I complex and ubiquitination govern endoplasmic reticulum to cell surface trafficking of the nicotinic acetylcholine receptor alpha-Subunit. J Biol Chem 2001; 276:18384-91.
33. Munster AK, Weinhold B, Gotza B, Muhlenhoff M, Frosch M, Gerardy-Schahn R. Nuclear localization signal of murine CMP-Neu5Ac synthetase includes residues required for both nuclear targeting and enzymatic activity. J Biol Chem 2002; 277:19688-96.
34. Fagerlund R, Melen K, Kinnunen L, Julkunen I. Arginine/lysine-rich nuclear localization signals mediate interactions between dimeric STATs and importin alpha 5. J Biol Chem 2002; 277:30072-8.
35. Bildl W, Strassmaier T, Thurm H, Andersen J, Eble S, Oliver D, Knipper M, Mann M, Schulte U, Adelman JP, Fakler B. Protein kinase CK2 is coassembled with small conductance Ca^{2+}-activated K^+ channels and regulates channel gating. Neuron 2004; 43:847-58.
36. Takahata T, Hayashi M, Ishikawa T. SK4/IK1-like channels mediate TEA-insensitive, Ca^{2+}-activated K^+ currents in bovine parotid acinar cells. Am J Physiol Cell Physiol 2003; 284:C127-44.
37. Xia XM, Fakler B, Rivard A, Wayman G, Johnson-Pais T, Keen JE, Ishii T, Hirschberg B, Bond CT, Lutsenko S, Maylie J, Adelman JP. Mechanism of calcium gating in small-conductance calcium-activated potassium channels. Nature 1998; 395:503-7.
38. Hirschberg B, Maylie J, Adelman JP, Marrion NV. Gating of recombinant small-conductance Ca-activated K^+ channels by calcium. J Gen Physiol 1998; 111:565-81.
39. Schumacher MA, Crum M, Miller MC. Crystal structures of apocalmodulin and an apocalmodulin/SK potassium channel gating domain complex. Structure 2004; 12:849-60.
40. Schumacher MA, Rivard AF, Bachinger HP, Adelman JP. Structure of the gating domain of a Ca2+-activated K+ channel complexed with Ca^{2+}/calmodulin. Nature 2001; 410:1120-4.
41. Hilgemann DW, Ball R. Regulation of cardiac Na^+, Ca^{2+} exchange and KATP potassium channels by PIP_2. Science 1996; 273:956-9.
42. Hilgemann DW. Cytoplasmic ATP-dependent regulation of ion transporters and channels: Mechanisms and messengers. Annual Review of Physiology 1997; 59:193-220.
43. Dong K, Tang L, MacGregor GG, Hebert SC. Localization of the ATP/phosphatidylinositol 4,5 diphosphate-binding Site to a 39-amino acid region of the carboxyl terminus of the ATP-regulated K^+ channel kir1.1. J Biol Chem 2002; 277:49366-73.
44. Prescott ED, Julius D. A modular PIP_2 binding site as a determinant of capsaicin receptor sensitivity. Science 2003; 300:1284-8.
45. Shyng SL, Cukras CA, Harwood J, Nichols CG. Structural determinants of PIP_2 regulation of inward rectifier KATP channels. J Gen Physiol 2000; 116:599-608.
46. Srivastava S, Li Z, Lin L, Liu G, Ko K, Coetzee WA, Skolnik EY. The phosphatidylinositol 3-phosphate phosphatase myotubularin- related protein 6 (MTMR6) is a negative regulator of the Ca^{2+}-activated K^+ channel KCa3.1. Mol Cell Biol 2005; 25:3630-8.
47. Srivastava S, Choudhury P, Li Z, Liu G, Nadkarni V, Ko K, Coetzee WA, Skolnik EY. Phosphatidylinositol 3-phosphate indirectly activates KCa3.1 via 14 amino acids in the carboxy terminus of KCa3.1. Mol Biol Cell 2006; 17:146-54.
48. Srivastava S, Li Z, Ko K, Choudhury P, Albaqumi M, Johnson AK, Yan Y, Backer JM, Unutmaz D, Coetzee WA, Skolnik EY. Histidine phosphorylation of the potassium channel KCa3.1 by nucleoside diphosphate kinase B is required for activation of KCa3.1 and CD4 T cells. Molecular Cell 2006; 24:665-75.